

## Microwave Assisted Solid State Synthesis of LiFePO<sub>4</sub>/C Using Two Different Carbon Sources.

Amol Naik<sup>1</sup>, Jian Zhou<sup>1\*</sup>, Chao Gao<sup>1</sup>, Lin Wang<sup>2</sup>

<sup>1</sup> State Key Laboratory of Advanced Technology for Materials Synthesis and Processing, Wuhan University of Technology, Wuhan- 430070, P. R. China

<sup>2</sup> Key Laboratory of Fiber Optic Sensing Technology and Information Processing, Ministry of Education, Wuhan University of Technology, Wuhan- 430070, P. R. China

\*E-mail: [jianzhou@whut.edu.cn](mailto:jianzhou@whut.edu.cn) Phone No.+86-27-87884448

Received: 17 June 2014 / Accepted: 7 August 2014 / Published: 25 August 2014

---

Nano size particles LiFePO<sub>4</sub>/C were prepared by a fast, facile, and environmentally friendly microwave-assisted solid-state reaction using different organic carbon sources. The particles are very uniform and are 100–300nm in size. The effects of the carbon sources on the microstructure and electrochemical properties of LiFePO<sub>4</sub>/C nanoparticles were investigated by X-ray diffraction, scanning electron microscopy, field emission scanning electron microscopy, electrochemical measurements and cyclic voltammetry. The results showed that the LiFePO<sub>4</sub>/C nanoparticles prepared from sucrose as carbon source, has good crystallinity and higher percentage of graphitic carbon, provided an initial discharge capacity of are 145.6, 140.5 and 122.4 mAhg<sup>-1</sup> at 0.1, 0.5 and 1.0C respectively, with excellent capacity retention. These advantages, coupled with the simple and effective preparation method, render LiFePO<sub>4</sub>/C nanoparticles attractive for practical and large-scale applications.

---

**Keywords:** Microwave-assisted, nano-particles, carbon source, graphitic carbon,

### 1. INTRODUCTION

The shortages of fossil fuel and the pollution of human survival environment promote the rapid development of solar, wind, hydropower and other clean sustainable energy. The intermittency of wind and solar energy makes mandatory large-scale energy storage as a complement to these alternative energy sources, and rechargeable batteries can provide both portable and stationary storage of the electrical energy generated from wind and radiant solar power. Lithium-ion batteries for their high specific capacity, long life and less pollution have become new energy storage candidates for power source of electric vehicles. Recently, lithium iron phosphate (LiFePO<sub>4</sub>) has been successfully developed as cathode material in lithium-ion battery with high security and long service life. Beside

that it grieves inherent disadvantages, namely the low electronic conductivity and low Li<sup>+</sup> diffusion rate. So the modification and morphology control of LiFePO<sub>4</sub> have become the research focus [1, 2].

During the past decade, nanomaterials have been used as electrode materials in lithium ion batteries, due of their diverse novel physicochemical and electrochemical properties [3]. The use of nanostructures (i.e., nanoscale size or nanoporous structures) has been widely investigated to improve Li<sup>+</sup> transport in electrodes by shortening the Li<sup>+</sup> insertion/extraction pathway. Now, the LiFePO<sub>4</sub> has been prepared by some methods, such as solid-phase and sol-gel methods [4, 5]. Among the synthesis methods for nanomaterials, low-heating solid-state reaction is a very simple and highly effective technique [3]. However, the reduction agent remains indispensable in the heat treatment process. The most commonly used reduction agents are organisms that can produce gases, such as hydrogen (H<sub>2</sub>), or gaseous hydrocarbons during their calcination [6], thereby reducing Fe<sup>3+</sup> to Fe<sup>2+</sup>. In addition, decomposition of the organism can result in the formation of carbonaceous deposits on the surface of the LiFePO<sub>4</sub> particles. Peng *et al.* [7] employed oxalic acid as reductant to obtain a LiFePO<sub>4</sub>/C composite with excellent performance from FePO<sub>4</sub>·2H<sub>2</sub>O. Yang *et al.* [8] prepared LiFePO<sub>4</sub>/C using glucose as a reducing agent and FePO<sub>4</sub>·2H<sub>2</sub>O as an iron source. Different organic acid molecules feature various decomposition mechanisms to form reducing intermediates, which can influence the properties of the LiFePO<sub>4</sub> composites obtained [9]. Thus, a complex carbon source may play a synergistic effect in LiFePO<sub>4</sub> synthesis, as reported by Hong *et al.* [10], who also observed that the morphology and electrochemical performance of the composites could be optimized by changing the ratio of sucrose to citric acid. Oh *et al.* [11] synthesized double carbon-coated LiFePO<sub>4</sub> with sucrose and pitch as the carbon source and reducing agent, respectively. Up to now, there are few papers that have reported the electrochemical properties of LiFePO<sub>4</sub>/C nanoparticles prepared from different organic carbon sources [12,13]. Our work is a first kind of attempt to prepare LiFePO<sub>4</sub> from iron source, which will produce reducing atmosphere itself throughout the sample bulk, along with different carbon sources. Nano particles size LiFePO<sub>4</sub>/C were prepared using two different organic carbon sources citric acid and sucrose along with iron source Fe<sub>2</sub>(CO)<sub>9</sub> by microwave-assisted solid-state reaction. Compared to conventional heating methods, microwave heating has the advantages of uniform, rapid, and volumetric heating, without sacrificing the quality of the product. The LiFePO<sub>4</sub>/C nanoparticles obtained by the proposed method had a very uniform particle size distribution. The microstructure, morphology, and electrochemical performance of the as synthesized products were investigated systematically.

## 2. EXPERIMENTAL

### 2.1 Synthesis of LiFePO<sub>4</sub>/C

LiFePO<sub>4</sub>/C composites were prepared by microwave assisted solid-state reaction, to investigate the effects of different organic carbon sources on the electrochemical performance of the LiFePO<sub>4</sub>/C. LiFePO<sub>4</sub> samples were prepared by heating mixture of LiOH (99% SCR, Shanghai, China), NH<sub>4</sub>H<sub>2</sub>PO<sub>4</sub> (99% SCR, Shanghai, China), Fe<sub>2</sub>(CO)<sub>9</sub> (99%, Jiangsu Tianyi Ultra-Fine Metal Powder Co. Ltd, Jiangsu, China) along with different organic compounds [citric acid or sucrose (99% SCR, Shanghai,

China)] in single mode microwave heating system. The stoichiometric mixture of  $\text{NH}_4\text{H}_2\text{PO}_4$  and  $\text{Fe}_2(\text{CO})_9$  were mixed in agate mortar and ground with pestle for 30 minutes. The homogeneous mixture form is heated in oven at  $80^\circ\text{C}$  for further reaction. After 10 minutes of heating  $\text{LiOH}$  and citric acid (or sucrose) were added and ground thoroughly for another 30 minutes. The obtained material was ball milled for 15 hours in ethanol and then dried at  $70^\circ\text{C}$  in oven to get free flowing powder, which was compressed (12MPa) to pellets and heated in sealed quartz crucible. The microwave irradiation for both the mixtures was performed in a specially designed single mode microwave furnace at 2.45GHz and 136W for 8 minutes.

The two samples obtained after microwave treatment are here after named LF-1 (sample with 2.50mmol citric acid) and LF-2 (sample with 1.25mmol sucrose).

## 2.2 Characterization of $\text{LiFePO}_4/\text{C}$ synthesized

The crystalline phase of the resulting material was analyzed by powder X-ray diffraction (PANalytical X'Pert Pro) which was carried out using  $\text{Cu K}\alpha$  radiation ( $\lambda = 1.54056\text{\AA}$ ). Data were collected from 10 to 80 in  $2\theta$ , with a step size of 0.017 and 1.0s per step. The morphology of the product was observed by scanning electron microscope (JSM-5610LV) of powder sample whereas surface of the compress pellet was analyzed by Hitachi field-emission scanning electron microscopy (FE-SEM S-4800). The Raman spectroscopy (INVIA RENISHAW laser Raman spectroscope) analysis was performed with a system utilizing 632.5nm incident radiation and a  $50\times$  aperture (N. A.=0.75) resulting approximately a  $2\mu\text{m}$  diameter sampling cross section.

## 2.3 Electrochemical measurements

A cathode working electrode for electrochemical testing was prepared by mixing the product with acetylene black and 5% solution of polytetrafluoroethylene (PTFE) in water, with weight ratio 80:10:10. The slurry was prepared by using isopropyl alcohol and coated on thin aluminium sheet and drying in vacuum oven at  $120^\circ\text{C}$  for 24 h. Lithium foil was used as an anode, and 1M solution of  $\text{LiPF}_6$  in mixture of ethylene carbonate and dimethylene carbonate (1:1 v/v as electrolyte. These three parts were assembled into a 2025 type coin cell in an argon filled glove box at room temperature. The two electrodes were held apart with separator (Celgard No 2402). Charge-discharge characteristic of the sample was cycled between 2.7 to 4.2V by using battery test system (LAND CT2001A) at ambient temperature.

# 3. RESULT AND DISCUSSION

## 3.1 Phase structure and morphology.

Fig.1 displays the XRD patterns of the as-synthesized  $\text{LiFePO}_4/\text{C}$  composites. The powders obtained by using different organic carbon sources have very similar diffraction peaks to those of pure

orthorhombic olivine. The sample prepared from citric acid shows progressive shift towards higher angle.

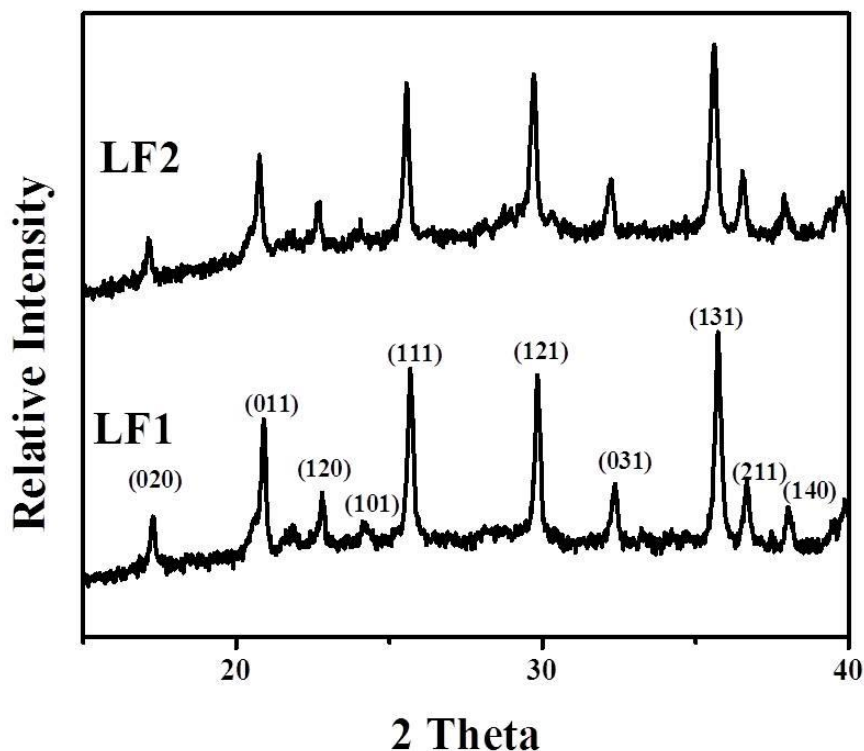


**Figure 1.** X-ray diffraction pattern of  $\text{LiFePO}_4/\text{C}$  samples.

All of the diffraction peaks match with the standard data for pure  $\text{LiFePO}_4$  phase (PDF-40-1499). The peak in the region 17.08, 20.69, 22.60, 24.01, 25.45, 29.67, 32.18, 35.49, 36.45, 37.78 corresponds to (020), (011), (120), (101), (111), (121), (031), (131), (211), (140) plane respectively. This implies that the olivine structure of  $\text{LiFePO}_4$  was well maintained during the preparation process, regardless of the different organic carbon sources. On the other hand, the peak of carbon is not observed, indicating that the amount of carbon is less than detection limit of XRD or most of which is amorphous carbon. In fact, the TG-DTA studies reveal that the amounts of carbon in LF1 and LF2 are about 4.74 and 8.33wt% respectively. Though two different organic compounds (sucrose and citric acid), as carbon source, were mixed in the raw material, and the content of carbon as to  $\text{LiFePO}_4/\text{C}$  is maintained 8 wt% by calculation, the final content of carbon is different in LF1 and LF2. It might be attributable to the complicated preparation process. It is well known that the added carbon sources during the hydrothermal synthesis process would conduct some chemical reactions at  $\text{LiFePO}_4$  formation temperature, which offer a good dispersion and reducible environment for growth of  $\text{LiFePO}_4$  and contribute to well-formed crystal  $\text{LiFePO}_4$ . The carbon prevents the oxidation of  $\text{Fe}^{2+}$  to  $\text{Fe}^{3+}$  and hinders the appearance of impurity during high temperature.

Fig. 2 illustrated the typical SEM and FE-SEM image of the  $\text{LiFePO}_4/\text{C}$  powder synthesized from different carbon sources (LF1 and LF2). The morphology and size of  $\text{LiFePO}_4$  was confirmed

from corresponding SEM and FE-SEM images. It is evident from the FE-SEM that synthesized sample exhibits particles size ranging from 100-300nm. But particle size measurement data revealed that it contains larger particles having size around 1  $\mu\text{m}$ .

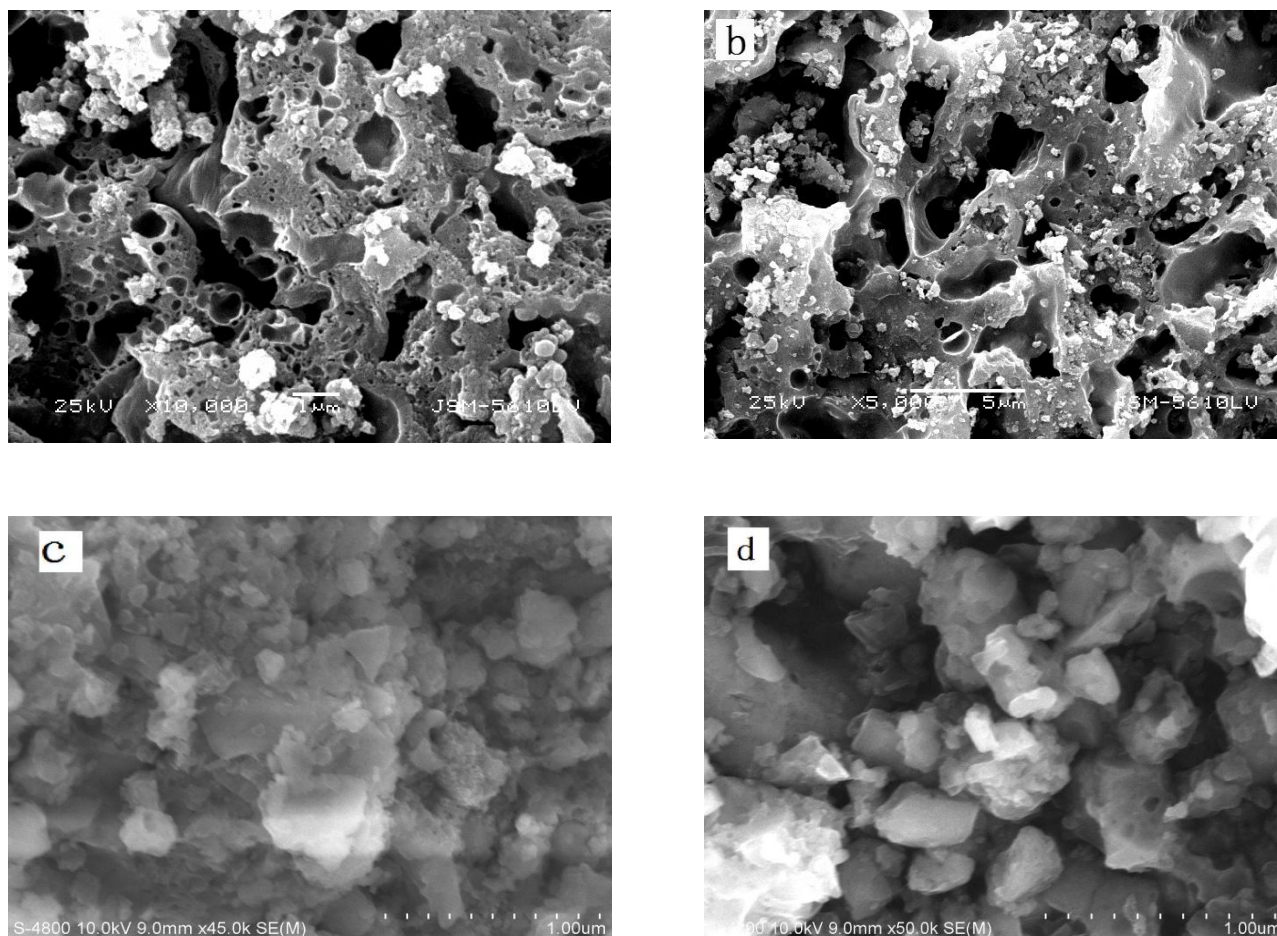


**Figure 2.** SEM micrographs of  $\text{LiFePO}_4/\text{C}$  a) LF1, b) LF2 FE-SEM of  $\text{LiFePO}_4/\text{C}$  c) LF1, d) LF2

SEM images exhibit that the such large particles are highly porous in both the cases and pores are uniformly spread over the bulk of the sample. It is also noted that the  $\text{LiFePO}_4/\text{C}$  prepared using citric acid has pores size less than 1  $\mu\text{m}$ , whereas sample produce by using sucrose has marginal larger pores. The formation of pores is due to evolution of gases during the decomposition of iron source  $\text{Fe}_2(\text{CO})_9$  and organic compound, which also take care of prevention of oxidation of  $\text{Fe}^{2+}$ . R Domink *et al* [14] reported that in porous  $\text{LiFePO}_4$  pore-to-pore distance determines the solid state diffusion of lithium; they also specified that such porous structure is only useful if the pores are decorated with an electronic conductor. In our work citric acid and sucrose are added as carbon source, which are on degradation produces, essential carbon necessary for coating of pores as well as nano crystalline  $\text{LiFePO}_4$  particles. Higher amount of carbon is advantageous, since it will produce well carbon coated  $\text{LiFePO}_4$ , with uniformly ornamented pores. Hence as the amount of carbon increases electrochemical

performance of the material should improve. But conductivity of the  $\text{LiFePO}_4/\text{C}$  composite depends upon the share of graphitic carbon, among the actual carbon deposited on the material.

3.2 Raman spectra

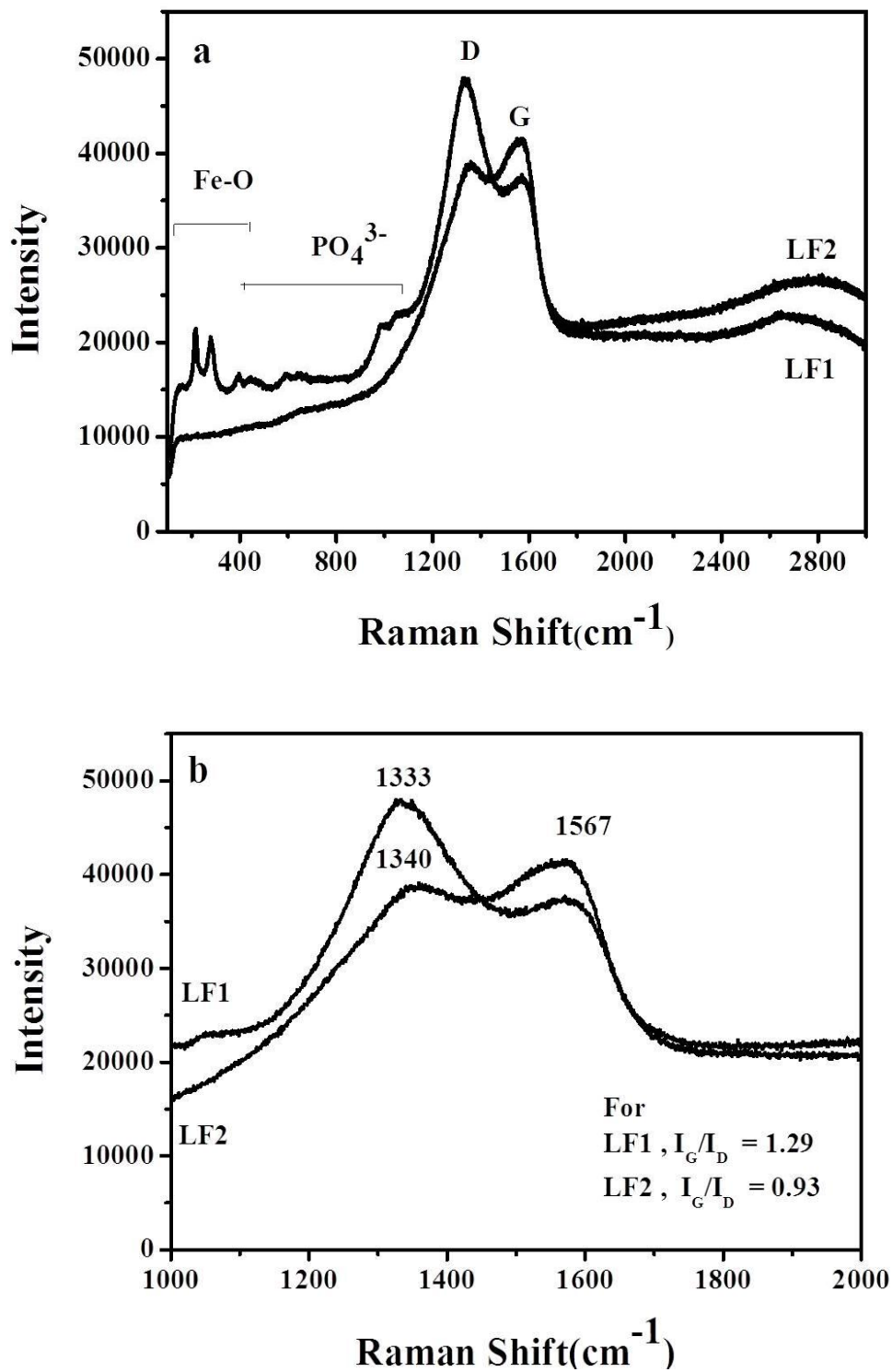
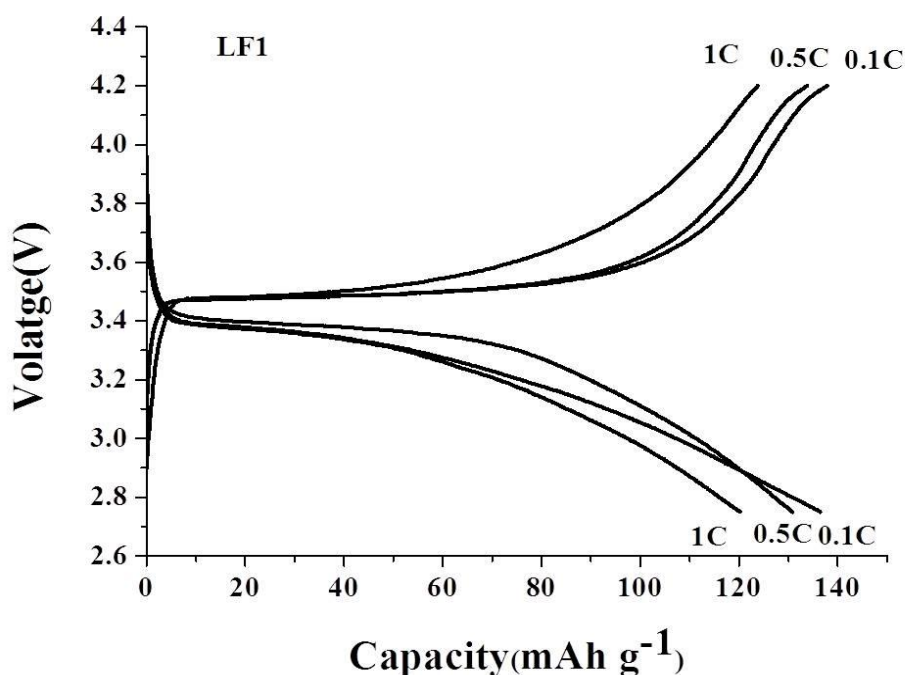


Figure 3. Raman spectra of  $\text{LiFePO}_4/\text{C}$

Raman spectrum recorded for carbon coated  $\text{LiFePO}_4$  prepared from different carbon sources are displayed in the Fig. 3. The carbon layer on  $\text{LiFePO}_4$  crystals makes it difficult to see the details of the spectrum of the olivine structure of  $\text{LiFePO}_4$  due to the attenuation of the signal and the overlapping of the spectral bands [15]. Due to lower concentration of carbon sample LF1 shows few peak corresponds to  $\text{PO}_4^{3-}$  and Fe-O. Two peaks at  $1336$  and  $1600\text{ cm}^{-1}$  correspond to the D and G bands of carbon, respectively. In case of LF2 typical bands was observed at  $1336$  and  $1601\text{ cm}^{-1}$  corresponding to D and G bands. The D band arises because of the disorder induced in  $\text{sp}^2$ -bonded carbon, whereas the G band arises from the in-plane vibration of  $\text{sp}^2$  carbon atoms [16,17]. However D and G bands of LF1 and LF2 were observed at  $1333$  and  $1567\text{ cm}^{-1}$ ,  $1340$  and  $1567\text{ cm}^{-1}$  respectively.  $I_D/I_G$  value (the peak intensity ratio between  $1336$  and  $1600\text{ cm}^{-1}$  peaks) generally provides a useful index to compare the degree of crystallinity of various materials, i. e. smaller the ratio of  $I_D/I_G$  higher the degree of carbon ordering in the material.  $I_D/I_G$  ratio of LF1 is 1.19, for LF2 it is decrease to 0.93. The higher intensity of G-band in LF2 sample indicate that the *in-situ* pyrolysis of sucrose produced more graphitic carbon than the decomposition of citric acid during microwave heating, which can improve the electrical conductivity of  $\text{LiFePO}_4/\text{C}$  powders.

### 3.3 Electrochemical properties of synthesized $\text{LiFePO}_4/\text{C}$

The initial charge-discharge performances of  $\text{LiFePO}_4/\text{C}$  (LF1 and LF2) at various charging rates are shown in the Fig.4. It can be seen from the figure that carbon sources have important effect on the charge-discharge performances of these  $\text{LiFePO}_4/\text{C}$  composites.



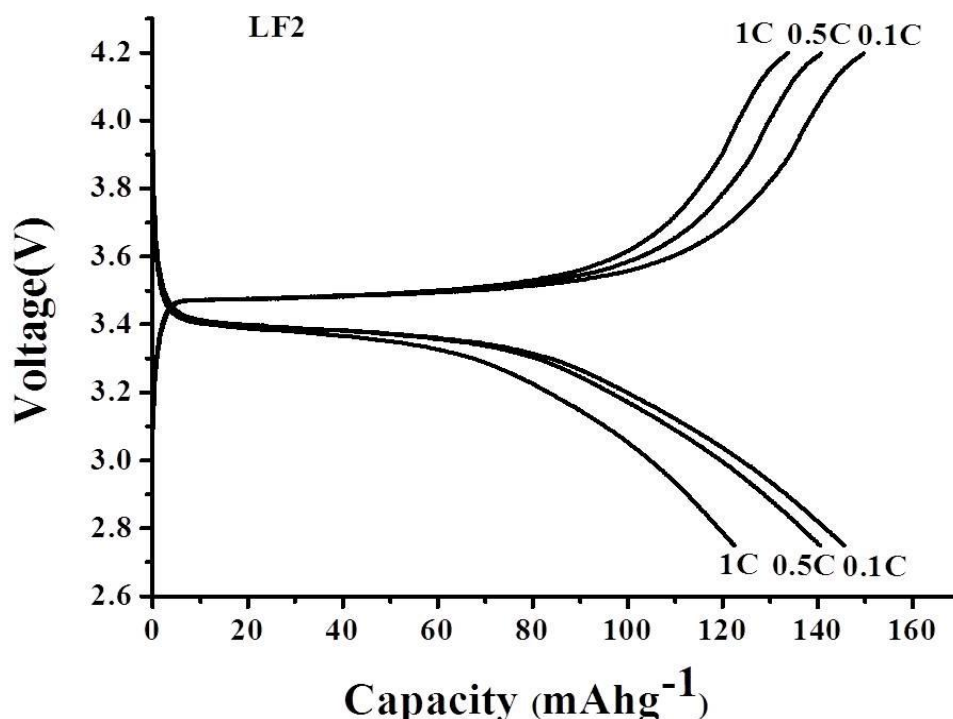


**Figure 4.** Initial charge-discharge curves of  $\text{LiFePO}_4/\text{C}$  at different charging rates.

The initial discharge capacities of LF1 were 136.4, 130.8 and 120.2  $\text{mAhg}^{-1}$  at charge-discharge rate of 0.1, 0.5 and 1.0C respectively. Sample LF2 prepared by sucrose as carbon source has maximum discharge capacities, which are 145.6, 140.5 and 122.4  $\text{mAhg}^{-1}$  at charge-discharge rate of 0.1, 0.5 and 1.0C respectively. All of the samples displayed flat charge and discharge voltage plateaus around 3.5 V and 3.4 V at a rate of 0.2 C, respectively. The capacity dropped with increasing C rate, indicating that the capacity loss was restricted by lithium-ion diffusion.

The cycling behaviors of different  $\text{LiFePO}_4/\text{C}$  nanoparticles are presented in Fig. 5. LF1 delivered an initial discharge capacity of 136.4, 130.8 and 120.2  $\text{mAh g}^{-1}$ , but after 50 charge-discharge cycle tests, its discharge capacity decrease to 133.1, 125.9 and 110  $\text{mAh g}^{-1}$  at charge-discharge rate 0.1, 0.5 and 1C respectively; as for LF2, its initial discharge capacity was 145.6, 140.5 and 122.4  $\text{mAhg}^{-1}$ , it decrease to 143.4, 131.7 and 115.3  $\text{mAhg}^{-1}$  after 50 charge/discharge cycles at rate 0.1, 0.5 and 1C respectively. Among these composites, LF2 has the highest initial discharge capacity, combined with excellent capacity retention; it may be due to more residual carbon and the high degree of graphitization of the carbon in the composite, which can improve the electrochemical performance of LF2. It is obvious that all the samples exhibit excellent reversibility due to their nanoparticles with excellent crystallinity, porous nature and carbon doping, which reduce the diffusion length of the ions in the sample and enhance the electronic conductivity.

The appropriate amount of carbon coated on a sample can improve its electrochemical properties [16]. However, the carbon from different carbon-containing compounds confers varying performance. Choosing the appropriate carbon precursor is very important in obtaining a  $\text{LiFePO}_4/\text{C}$

composite with excellent properties. In this work, sucrose could be used as an appropriate carbon precursor, given the beneficial effects of pyrolytic carbon to the  $\text{LiFePO}_4$  particles, including improved carbon structure, increased homogeneity of the resulting grains, and uniformity of the coated carbon layer on the particles.

Liu *et al.* [19] has done the similar type of studies using citric acid, PVA and glucose as carbon source by adopting hydrothermal route. They reported that,  $\text{LiFePO}_4/\text{C}$  synthesized with 5% glucose as carbon resource produces small particle size and even regular shape. They further quoted that, the initial discharge specific capacity  $151.2\text{mAhg}^{-1}$  and  $87.3\text{mAhg}^{-1}$  at 0.1C and 2C rate, respectively. In our investigation though we have attend marginally less initial discharge capacity, compare to Liu *et al.* our method is simple and does not require long heating duration and material obtained has better specific capacity retention even after 50 cycles.

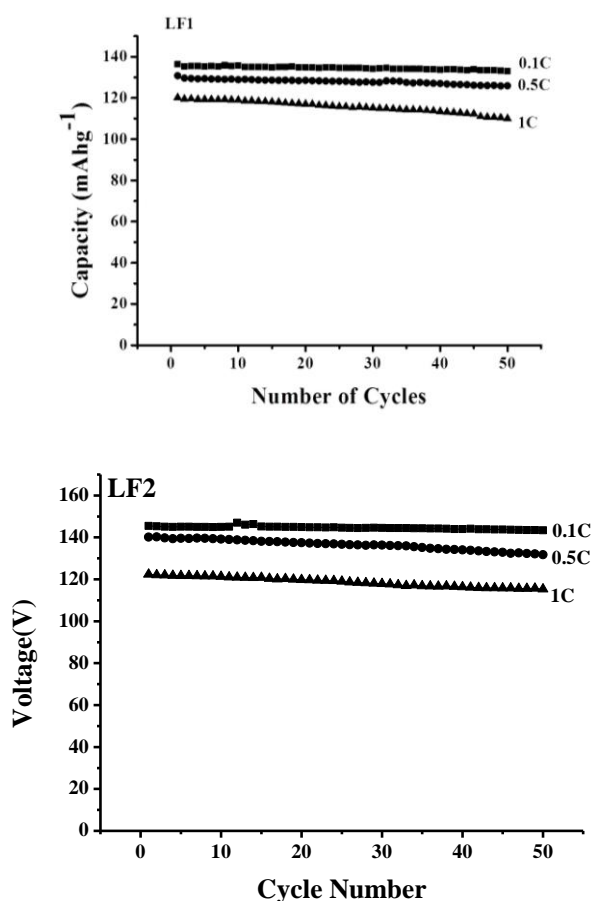


**Figure 5.** Reversible capacity during continuous cycling at 0.1, 0.5 and 1C (the cell was charge and discharge with the same current density)

#### 4. CONCLUSION

$\text{LiFePO}_4/\text{C}$  nanoparticles were synthesized using different organic carbon sources (citric acid and sucrose) by microwave-assisted solid-state reaction. In comparison to the conventional heating method, the microwave-assisted heat-treatment process is superior in terms of shorter reaction time

and more uniform particle size. The electrochemical measurement results indicated that the LiFePO<sub>4</sub>/C nanoparticles formed using sucrose as the carbon source had a high initial discharge capacity and minor capacity fading even after 50 charge/discharge cycles. Therefore, microwave-assisted solid-state reaction is an effective method to prepare LiFePO<sub>4</sub>/C nanoparticles, and sucrose is an effective carbon source to improve the electrochemical properties of LiFePO<sub>4</sub>. The good cycling stability and high discharge capability, coupled with the low cost and environmentally benign nature of iron, may make this cathode material attractive for large-scale applications.

#### ACKNOWLEDGEMENTS

The research was supported by Chinese National Science Foundation (51172175, 51072147) and Hubei Science & Technology Plan (2012FFB05107, 2013BKB006)

#### References

1. S. W. Oh, S. T. Myung, S. M. Oh, K. H. Oh, K. Amine, B. Scrosati, Y. K. Sun, *Adv. Mater.*, 22 (2010) 4842-4945.
2. K. Shiraishi, K. Dokko, K. Kanamura, *J. Power Sources*, 146 (2005) 555-558.
3. Y. Huang, R. Jiang, D. Jia, Z. Guo, *Mater. Lett.*, 65 (2011) 3486-3488.
4. X. D. Yan, G. L. Yang, J. Liu, *Electrochim. Acta*, 54 (2009) 5770-5774.
5. D. Choi, P. N. Kumta, *J. Power Sources* 163 (2007) 1064-1069.
6. N. Ravet, M. Gauthier, K. Zaghib, J. B. Goodenough, A. Mauger, F. Gendron, C.M. Julien, *Chem. Mater.* 19 (2007) 2595-2602.
7. W. X. Peng, L. F. Jiao, H. Y. Gao, Z. Qi, Q. H. Wang, H. M. Du, Y.C. Si, Y.J. Wang, H. T. Yuan, *J. Power Sources* 196 (2011) 2841-2847.
8. K. R. Yang, Z. H. Deng, J. S. Suo, *J. Power Sources* 201 (2012) 274-279.
9. K. Kim, Y. H. Cho, D. Kam, H. S. Kim, J. W. Lee, *J. Alloys Compd* 504 (2010) 166-170.
10. J. H. Hong, Y. F. Wang, G. He, M.Z. He, *Mater. Chem. Phys.* 133 (2012) 573-577.
11. S. W. Oh, S. T. Myung, S. M. Oh, K. H. Oh, K. Amine, B. Scrosati, Y. K. Sun, *Adv. Mater.* 22 (2012) 4842-4845.
12. Y. Liu, W. Zhang, J. Jiang, D. Ma, H. Wang, *J. Mat. Sci. and Eng. B* 2 (4) (2012) 255-259.
13. Y. Huang, L. Wang, D. Jia, S.J. Bao, Z. Guo, *J. Nanopart. Res.* 15 (2013) 1459-1463
14. R. Dominko, M. Bele, M. Gaberscek, M. Remskar, D. Hanzel, J.M. Goupil, S. Pejovnik, J. Jamnik, *J. Power Sources*, 153 (2006) 274-280.
15. A. S. Anderson, J. O. Thomas, *J. Power source*, 108 (2002) 8-12
16. K. Zaghib, K. Striebel, A. Gueli, J. Shim, M. Armand, M. Gauthier, *Electrochim. Acta*, 50 (2004) 263-270.
17. N. J. Yun, H. W. Ha, K. H. Jeong, H. Y. Park, K. Kim, *J. Power Sources*, 160 (2006) 1361-1368.
18. H. Huang, S. C. Yin, L. F. Nazar, *Electrochem. Solid State* 4 (2001) A170-172.
19. Yuwen Liu, Wei Zhang, Jingna Jiang, Dongxing Ma and Haiyan Wang, *J. Mat. Sci. and Eng. B* 2 (4) (2012) 255-260